Distributed Optimal Control of Energy Hubs for Micro-Integrated Energy Systems

Qu, M.; Ding, T.; Jia, Wenhao; Zhu, Shanying; Yang, Y.; Blaabjerg, F.

Published in:
IEEE Transactions on Systems, Man, and Cybernetics: Systems

DOI (link to publication from Publisher):
10.1109/TSMC.2020.3012113

Publication date:
2021

Distributed Optimal Control of Energy Hubs for Micro-Integrated Energy Systems

Ming Qu, *Student Member, IEEE*, Tao Ding, *Senior Member, IEEE*, Wenhao Jia, *Student Member, IEEE*, Shanying Zhu, *Member, IEEE*, Yongheng Yang, *Senior Member, IEEE*, and Frede Blaabjerg, *Fellow, IEEE*

***Abstract*—Integrated energy systems become more and more important to realize the energy complementary property. Micro-integrated energy system, served as the terminal integrated energy system, will have the electricity delivered directly to the local customers by energy hubs (EHs). Here, the data and information of the EHs during the operation are confidential and should be kept by each owner. Therefore, this article designs a dual-decomposition-based distributed algorithm to address this problem, where the optimal consensus problem is used for the dual problem to update the multipliers. The primary and dual problems are alternatively solved until the Karush–Kuhn–Tucher condition is satisfied. For the proposed distributed algorithm, the feasibility can be strictly guaranteed during the iteration process. Moreover, theorems and lemmas are proved for the linear convergence rate. The numerical results verify the effectiveness of the proposed algorithm.**

***Index Terms*—Distributed optimal control, dual decomposition (DD), energy hubs (EHs), micro-integrated energy systems (m-IESs).**

NOMENCLATURE

Parameters

$\mathcal{V}$ Offset of all m energy hubs $\{1, 2, \ldots, m\}$.
m Number of energy hubs.
$\mathbf{B}$ Constraint matrix in the optimal exchange problem.
$\mathbf{O}$ Zero matrix with proper dimension.
I Identity matrix with proper dimension.
$\mathbf{W}$ Weight matrix of the communication network with elements ω_{ij}.
$\mathbf{1}$ Column vector with all elements 1 with proper dimension.
ρ Spectral radius of a matrix.
η_0 Connectivity of $\mathbf{W}$.
$\mathbf{0}$ Column vector with all elements 0 with proper dimension.
$\mathbf{T}$ Communication matrix used in the optimal consensus problem.
$\underline{\xi}\,()$ Eigenvalues of a matrix.
$\overline{\mathcal{R}}$ Extended real number set that equals the set of real numbers $\mathcal{R} \cup \{\pm\infty\}$.
$\mathcal{H}$ Euclidean space.
r Rank of a matrix.
$\mathbf{A}_i$ Transformation matrix of the energy hub.
P_L, H_L, G_L Total electricity, heat, and gas load demands.
$\underline{P_i^{\text{out}}}$, $\underline{H_i^{\text{out}}}$, $\underline{G_i^{\text{out}}}$ Lower bound of the ith energy hub for electricity, heat, and gas.
$\overline{P_i^{\text{out}}}$, $\overline{H_i^{\text{out}}}$, $\overline{G_i^{\text{out}}}$ Upper bound of the ith energy hub for electricity, heat, and gas.

Variables

C Total cost of the micro integrated energy system.
C_i^P Local cost of the energy hub to purchase power.
C_i^H Local cost of the energy hub to purchase heat.
C_i^G Local cost of the energy hub to purchase natural gas.
P_i^{in} Amount of power purchased by the energy hub, whose collection vector is $\mathbf{P}^{\text{in}}$.
H_i^{in} Amount of heat purchased by the energy hub, whose collection vector is $\mathbf{H}^{\text{in}}$.
G_i^{in} Amount of natural gas purchased by the energy hub, whose collection vector is $\mathbf{G}^{\text{in}}$.
P_i^{out} Power output of the energy hub, whose collection vector is $\mathbf{P}^{\text{out}}$.
H_i^{out} Heat output of the energy hub, whose collection vector is $\mathbf{H}^{\text{out}}$.
G_i^{out} Natural gas output of the energy hub, whose collection vector is $\mathbf{G}^{\text{out}}$.
$\boldsymbol{\lambda}$ Dual variable introduced to local cost function.
$\mathbf{y}_i$ Duplicated variable of $\boldsymbol{\lambda}$.
$\mathbf{y}$ Collection vector of all $\mathbf{y}_i$ that is structure as $[\mathbf{y}_1^T, \mathbf{y}_2^T, \ldots, \mathbf{y}_m^T]^T$.

Manuscript received March 7, 2020; revised May 13, 2020; accepted July 13, 2020. This work was supported in part by the National Key Research and Development Program of China under Grant 2016YFB0901900; in part by the National Natural Science Foundation of China under Grant 51977166; in part by the China Postdoctoral Science Foundation under Grant 2017T100748; in part by the Natural Science Foundation of Shaanxi Province under Grant 2020KW-022; and in part by the CURENT Research Center. This article was recommended by Associate Editor T. I. Strasser. *(Corresponding author: Tao Ding.)*

Ming Qu, Tao Ding, and Wenhao Jia are with the Department of Electrical Engineering, Xi'an Jiaotong University, Xi'an 710049, China (e-mail: tding15@mail.xjtu.edu.cn).

Shanying Zhu is with the Department of Automation, Shanghai Jiao Tong University, Shanghai 200240, China.

Yongheng Yang and Frede Blaabjerg are with the Department of Energy Technology, Aalborg University, 9220 Aalborg, Denmark.

Color versions of one or more of the figures in this article are available online at http://ieeexplore.ieee.org.

Digital Object Identifier 10.1109/TSMC.2020.3012113

$\mathbf{x}_i$	Shifted local decisive variable of the ith energy hub.
$\mathbf{x}$	Collection vector of all $\mathbf{x}_i$ that is structure as $\left[\mathbf{x}_1^T, \mathbf{x}_2^T, \ldots, \mathbf{x}_m^T\right]^T$.
$\mathbf{z}_i$	Auxiliary variable for the ith EH.
f	Total objective function of the primary model.
f_i^0	Cost function of the ith EH.
f_i	Convex and differentiable part of the ith EH.
t_i	Regularization term of the ith EH.
f_i^1	Cost function of electricity for the ith EH.
f_i^2	Cost function of heat for the ith EH.
f_i^3	Cost function of natural gas for the ith EH.
a_i, b_i	Coefficients for cost function of electricity for the ith EH.
c_i, d_i	Cost function coefficients of heat for the ith EH.
e_i, f_i	Cost function coefficients of natural gas for the ith EH.
f^*	Optimal value of the primary model.
x^*	Optimal solution of the primary model.
y^*	Optimal dual solution of the primary model.

I. Introduction

A. Background

OVER the past few decades, the climate change and the overspend of fossil energy have put a great challenge on the development of sustainable energy. According to the World Energy Congress, it is estimated that the ultimate amount of traditional fossil fuels (coal, oil, and natural gas), which accounts for 80% of the world's current energy consumption, is expected to sustain for two hundred years and cannot meet the rapidly growing energy consumption of society. To address this challenge, the development of integrated energy system (IES) has provided an opportunity [1], [2], which combines several different kinds of energy systems (such as electrical power system, natural gas system, and district heating system) together to improve the energy utilization efficiency. As a result, the IES has aroused a wide concern from government, enterprise, and scholars, due to its benefits in terms of low carbon footprint, economics, flexibility, reliability and sustainability.

Note, IESs have two structures with respect to different system levels. For the transmission system level, IES mainly contains electricity and natural gas without heat energy. This is because heat cannot be transferred over long distances and should be balanced locally. For the distribution system level, a micro-IES (m-IES), which is typically used for a local community residential supply, will contain heating resources in addition to the electricity and natural gas.

In order to tightly couple the different forms of energy resources in the IES, a component is needed to achieve the production, conversion, storage, and consumption of different energy carriers, which is called as energy hub (EH). For example, thermoelectric converters, pumps, and electric boilers realize the coupling of electric energy and heating energy; power-to-gas devices (P2Gs) and gas turbines realize the coupling of electric energy and natural gas [3], [4]; combined heat and power (CHP) units realize the coupling of electric energy, thermal energy, and natural gas [5], [6]. In general, EHs are the core equipment for the interaction of different energy carriers in the IES, so the modeling of EHs is critical. Mohammad *et al.* [7] reviewed several models of the EH and discussed the corresponding strengths and weaknesses of each model. Based on the modeling of EHs, many techniques have been developed for the IES to improve the energy efficiency of the whole energy systems, fully accommodate renewable energy, enhance the energy transformation flexibility, etc.

B. Literature Reviews

IES and m-IES have been studied extensively, especially in unified energy flow, economic dispatch, and optimal energy flow (OEF). Accurately and effectively analyzing the energy flow is of great significance to the operations, planning, and control of IESs. Various methods were proposed to execute the energy-efficiency-based control architectures and algorithms in [8]–[10]. With the rapid development of renewable energy, a unified energy flow framework considering wind power and other renewable energy has been established in [11]. Obviously, renewable energy will bring uncertainties to power generation, which will affect the operation of the gas network and the heat network as well. Chen *et al.* [12], Hu *et al.* [13], and Aien *et al.* [14] established the probabilistic analysis models for computing the IES energy flow evaluate the impact from uncertainties.

Based on the analysis of energy flow, OEF is studied to improve the energy efficiency and reduce the cost. Andebili and Shen [15] focused on a bi-level optimization-based energy scheduling for m-IES. The price-controlled strategy was implemented to coordinate the energy management between smart homes and generation companies. Furthermore, Faqiry and Das [16] investigated an energy auction mechanism by microgrid controller between buyers and sellers. Also, the physical grid constraints were addressed in the optimization model and the buyers' private information can be preserved. Additionally, the economic dispatch model for an m-IES was established in [17] that quantitatively analyzed the influence of the integrated demand response on wind power utilization.

In addition to the economic dispatch, OEF is also a hot topic to optimize the energy flow subject to the security constraints. Shao *et al.* [19] proposed a state variable-based EH model which avoided the nonlinearity induced by dispatch factors, so that the OEF of combined power and gas systems can be formulated as an MILP model. Shabanpour-Haghighi and Seifi [20] gave a modified teaching–learning-based optimization method to solve the multiperiod OEF problem of multicarrier energy networks. With the consideration of different response time horizons of the gas and power systems, Fang *et al.* [21] formulated a dynamic OEF model and transformed it into a single-stage linear programming. A multiperiod probabilistic OEF model was designed in [22], which adopted three-point estimation method to solve the uncertainty caused by wind power and load prediction. From the perspective of reducing carbon emission, the stochastic OEF for an m-IES with energy storage was studied in [23] to handle uncertainties in energy demand and renewable generation.

Note that all the above studies were performed by using centralized approaches, which require a center to handle the whole network information. However, since different EHs in an m-IES may belong to different companies, the centralized approaches cannot guarantee privacy concerns on sensitive data, for example, the energy prices of different companies reflected by the gradient information. Thus, the decentralized approaches (also known as, the distributed optimization methods) is necessary to protect the information privacy of different EH agents.

In fact, distributed optimization methods for solving economic dispatch, unit commitment, and OEF have attracted considerable attentions in recent research. Wang *et al.* [24] developed an optimization model and blockchain-based architecture to manage the operation of crowdsourced energy systems to solve the day-ahead scheduling problem of generation and controllable distributed energy resources. The presented operational model can also be used to operate islanded microgrids. Furthermore, a peer-to-peer distributed coordination method was considered in [25] for optimizing the cyber-physical energy system. Then, a fully distributed algorithm was designed to exchange local information only among neighbors without the interactive information between generation and load.

However, the augmented Lagrange methods may result in the inseparable problem. Thus, ADMM was used to conquer this trouble [26], [27]. Ma *et al.* [28] reviewed several calculation forms of ADMM in distributed power systems and compared the differences between consensus ADMM and proximal ADMM in economic scheduling problems. In addition, a fully distributed and robust algorithm based on ADMM was applied to solve OPF problem in [29], and this algorithm did not need a coordination center. Considering stochastic communication delay and aiming at the minimum power loss, Xu *et al.*[30] raised a synchronous and asynchronous method to solve the distributed OPF problem. More specifically, Bolognani and Zampieri [31] verified the computational efficiency of the distributed algorithm ADMM to solve the economic dispatch problem through a large-scale Polish 2383-bus system.

Despite the improvements of the aforementioned distributed algorithms, they have two common disadvantages.

1) The convergence of the ADMM method is challenging. Chen *et al.* [32] pointed out that the convergence of the ADMM is not necessarily guaranteed for the multiblock convex optimization problem while only the case with two blocks can be convergent. Meanwhile, some counterparts were illustrated which greatly challenged the ADMM for the applications using distributed optimization.
2) ADMM algorithms always terminated when the feasibility was met, which means that if the iteration was interrupted by unexpected failures, the solution could not be feasible (or the infeasible solution will be obtained during the iteration process).

In view of this, the algorithm has been studied which not only solves both the primal problem and the dual problem simultaneously but also ensures that each step is feasible. Under assumptions that the objective function has strong convexity and smoothness, Doan and Olshevsky [33] proposed a fully distributed primal–dual method, which can achieve a geometric convergence. Based on this idea, Qu and Li [34] raised a distributed algorithm which can accelerate the convergence by using history information to achieve fast and accurate estimation of the average gradient. Xu *et al.* [35] focused on different constant step-sizes and developed an augmented distributed gradient method based on consensus theory. It had been proved that the optimal solution could be obtained even when the step size was constant. Furthermore, Xu *et al.* [36] created the distributed forward–backward Bregman splitting algorithm which was suitable for stochastic networks by solving both primal and dual problem simultaneously. In consideration of privacy, a distributed method called dual splitting approach (DuSPA) was established in [36], which did not need to communicate iterative information when seeking optimal value. This method was proven to have a linear convergence rate for smooth and strongly convex cost functions.

C. Contributions

We propose a novel distributed algorithm for EH optimal control in m-IES, which does not need to exchange the sensitive information of different types of energy resources, thus keeping the data privacy [37], [38] as the ADMM method. Specifically, the main contributions of this article can be summarized as follows.

1) A dual-decomposition (DD)-based distributed algorithm is proposed for optimal dispatching the m-IES in which the feasibility can be strictly guaranteed at each step. The optimal consensus problem (OCP) is used for the dual problem to update the multipliers. The primary and dual problems are alternatively solved until the KKT condition is satisfied.
2) We investigate the structure of the communication network matrix for the m-IES and the properties of the communication network matrix are given to guarantee the convergence. In particular, we have strictly proven the linear convergence rate of the proposed method on the economic dispatch model under the mild condition that the objective function is smooth and strongly convex.

The reminder structure of this article is as follows. Section II develops the basic optimal control model for m-IESs, and the model is rewritten as an optimal exchange problem (OEP) form. Section III describes the DD algorithm which contains: 1) the communication network model; 2) the dual optimal consensus model; and 3) the specific process of the DD algorithm. Section IV proves the linear convergence rate of the proposed method under the mild conditions. Section V shows the results

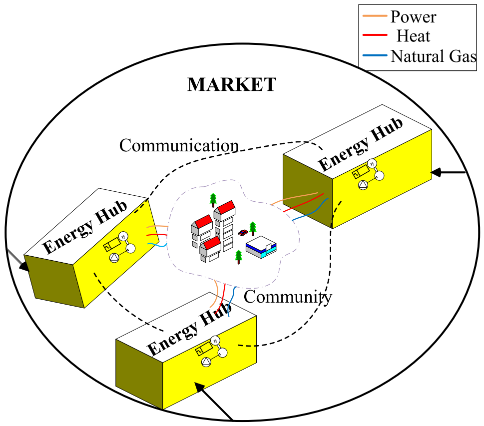

Fig. 1. m-IES with multiple EHs.

and analysis of case studies. Finally, Section VI draws main conclusions.

II. Optimal Control Model for Micro Integrated Energy Systems

Consider that the integrated load demands in an m-IES are supplied by several EHs, including electricity, heat, and natural gas. As shown in Fig. 1, the local output of each individual EH is limited for different energy resources due to the physical constraints and the input purchases electricity, heat, and natural gas from the external price-based markets. The EH itself will convert the energy resources from one type to another type, such that the output quantities of the energy resources will meet the total load demands while satisfying the physical constraints. Furthermore, the optimization model for the optimally controlling EHs of an m-IES is set up to minimize the total purchasing cost for the whole m-IES while satisfying the energy balance constraints for each energy resource as well as the physical constraints for EHs, such that

$$\min_{\mathbf{P},^{\text{in}}\mathbf{H}^{\text{in}},\mathbf{G}^{\text{in}},\mathbf{P}^{\text{out}},\mathbf{H}^{\text{out}},\mathbf{G}^{\text{out}}\in\mathbf{R}^m} C\left(\mathbf{P}^{\text{in}},\mathbf{H}^{\text{in}},\mathbf{G}^{\text{in}}\right) = \sum_{i=1}^{m}\left(C_i^P\left(P_i^{\text{in}}\right)+C_i^H\left(H_i^{\text{in}}\right) + C_i^G\left(G_i^{\text{in}}\right)\right) \tag{1}$$

$$\text{s.t. } \mathbf{A}_i\begin{pmatrix}P_i^{\text{in}}\\H_i^{\text{in}}\\G_i^{\text{in}}\end{pmatrix}=\begin{pmatrix}P_i^{\text{out}}\\H_i^{\text{out}}\\G_i^{\text{out}}\end{pmatrix}\quad\forall i\in\mathcal{V} \tag{2}$$

$$\sum_{i=1}^{m}P_i^{\text{out}}=P_L\quad\forall i\in\mathcal{V} \tag{3}$$

$$\sum_{i=1}^{m}H_i^{\text{out}}=H_L\quad\forall i\in\mathcal{V} \tag{4}$$

$$\sum_{i=1}^{m}G_i^{\text{out}}=G_L\quad\forall i\in\mathcal{V} \tag{5}$$

$$\underline{P_i^{\text{out}}}\le P_i^{\text{out}}\le\overline{P_i^{\text{out}}}\quad\forall i\in\mathcal{V} \tag{6}$$

$$\underline{H_i^{\text{out}}}\le H_i^{\text{out}}\le\overline{H_i^{\text{out}}}\quad\forall i\in\mathcal{V} \tag{7}$$

$$\underline{G_i^{\text{out}}}\le G_i^{\text{out}}\le\overline{G_i^{\text{out}}}\quad\forall i\in\mathcal{V} \tag{8}$$

where $\mathbf{A}_i$ in (2) is a $\overline{\mathcal{R}}^{3\times 3}$ matrix that describes the relationship between the output and input of the EH i; $\overline{\mathcal{R}}$ is the real number space; Constraints (3)–(5) are the energy balance for each kind of energy resource; and constraints (6)–(8) limit the output of the EHs.

It should be noted that in the practical engineering, the cost response function is considered to be quadratic. Therefore, the cost functions ($C_i^P(\bullet)$, $C_i^H(\bullet)$, $C_i^G(\bullet)$) are usually expressed as quadratic functions with positive coefficients, which have the strictly convex quadratic property [40], such that

$$C_i\left(P_i^{\text{in}},H_i^{\text{in}},G_i^{\text{in}}\right)=a_i\left(P_i^{\text{in}}\right)^2+b_iP_i^{\text{in}}+c_i\left(H_i^{\text{in}}\right)^2 + d_iH_i^{\text{in}}+e_i\left(G_i^{\text{in}}\right)^2+f_iG_i^{\text{in}}\quad\forall i\in\mathcal{V}. \tag{9}$$

Recall that the model (1)–(8) has a special mathematical structure where the constraints (2) and (6)–(8) are separable for each individual EH while only the equality energy balance constraints (3)–(5) will link multiple EHs together. Let $\mathbf{x}_i$ be the local decision variables of each EH, such that $x_i=(P_i^{\text{in}},H_i^{\text{in}},G_i^{\text{in}},P_i^{\text{out}},H_i^{\text{out}},G_i^{\text{out}})$. Splitting the constraints that only related to the local variables from the coupled constraints, we will encode the constraints (2) and (6)–(8) to the Euclidean space

$$\mathcal{H}=\left\{\begin{array}{c}\mathbf{A}_i\begin{pmatrix}x_{6i-5}\\x_{6i-4}\\x_{6i-3}\end{pmatrix}=\begin{pmatrix}x_{6i-2}\\x_{6i-1}\\x_{6i}\end{pmatrix}\\ \underline{P_i^{\text{out}}}\le x_{6i-2}\le\overline{P_i^{\text{out}}}\\ \underline{H_i^{\text{out}}}\le x_{6i-1}\le\overline{H_i^{\text{out}}}\\ \underline{G_i^{\text{out}}}\le x_{6i}\le\overline{G_i^{\text{out}}}\end{array}\right.\quad\forall i\in\mathcal{V}.$$

Then, shifting the energy load demands to zero by [36], the proposed optimal control model for m-IES can be recognized as the classical OEP as follows:

$$\min_{\mathbf{x}\in\mathcal{H}} f(\mathbf{x}):=\sum_{i=1}^{m}f_i^0(\mathbf{x}_i)=\sum_{i=1}^{m}(f_i(\mathbf{x}_i)+t_i(\mathbf{x}_i)) := \sum_{i=1}^{m}\left(f_i^1(x_{6i-5})+f_i^2(x_{6i-4})+f_i^3(x_{6i-3})+t_i(\mathbf{x}_i)\right) \tag{10}$$

$$\text{s.t. }\sum_{i=1}^{m}x_{6i-2}=0\quad\forall i\in\mathcal{V} \tag{11}$$

$$\sum_{i=1}^{m}x_{6i-1}=0\quad\forall i\in\mathcal{V} \tag{12}$$

$$\sum_{i=1}^{m}x_{6i}=0\quad\forall i\in\mathcal{V} \tag{13}$$

where the local cost function for the ith EH, giving $f_i:\mathcal{H}\to\overline{\mathcal{R}}$ is convex, differentiable, and is only related to the ith EH; the regularization term $t_i:\mathcal{H}\to\overline{\mathcal{R}}$ is convex but may be nonsmooth, which contains all the information related to the feasible region of the original optimization model. Obviously, $f_i^0(\cdot) = f_i(\cdot) + t_i(\cdot)$, for all i.

In a compact form, the primal OEP (*primal problem*) (10)–(13) can be rewritten as

$$\min_{\mathbf{x}\in\mathcal{H}} f(\mathbf{x}) := \sum_{i=1}^{m} f_i^0(\mathbf{x}_i) \tag{14}$$

$$\text{s.t. } \mathbf{B}^T\mathbf{x} = \mathbf{0} \tag{15}$$

where $\mathbf{B}^T = \begin{bmatrix} & & \mathbf{O}_{3\times 6m} & & \\ \mathbf{O}_{3\times 3} & \mathbf{I}_{3\times 3} & \cdots & \mathbf{O}_{3\times 3} & \mathbf{I}_{3\times 3} \end{bmatrix}$.

III. Dual-Decomposition-Based Distributed Algorithm

At first, it can be easily found that the OEP problem (14), (15) for the m-IES is a centralized optimization model that needs a control center to collect all the data from each EH. In order to conduct the OEP model in a distributed way, we will investigate the dual problem and relevant algorithm of the OEP to obtain the optimal solution in a distributed way. At the beginning, some preliminaries should be given.

A. Preliminaries

1) Spectral Radius: The spectral radius $\rho(\mathbf{A})$ of the matrix $\mathbf{A}$ is defined as

$$\rho(\mathbf{A}) = \max\{|\xi(\mathbf{A})|\} \tag{16}$$

where ξ represent the eigenvalues of $\mathbf{A}$.

*2) **G**-Space:* A $\mathbf{G}$-space is defined by the given symmetric positive-definite matrix $\mathbf{G}$ with the induced norm as follows:

$$\langle \boldsymbol{\alpha}, \boldsymbol{\beta}\rangle_{\mathbf{G}} = \langle \mathbf{G}\boldsymbol{\alpha}, \boldsymbol{\beta}\rangle \text{ and } \|\boldsymbol{\alpha}\|_{\mathbf{G}} = \sqrt{\langle \mathbf{G}\boldsymbol{\alpha}, \boldsymbol{\alpha}\rangle} \quad \forall \boldsymbol{\alpha}, \boldsymbol{\beta} \in \mathcal{H}. \tag{17}$$

3) Saddle Point: A saddle point of ϕ in the domain $\mathcal{D}$ is the pair (x^*, y^*) that satisfies the following condition:

$$\phi\big(x^*, y\big) \le \phi\big(x^*, y^*\big) \le \phi\big(x, y^*\big) \quad \forall (x, y) \in \mathcal{D}. \tag{18}$$

4) Fenchel Duality: Let $f : \mathcal{H} \to \overline{\mathcal{R}}$ be a convex function. Then, its convex conjugate (Fenchel' dual) is defined as

$$f^*(\mathbf{y}) = \sup_{\mathbf{x}\in\mathcal{H}}\{\langle \mathbf{x}, \mathbf{y}\rangle - f(\mathbf{x})\} \tag{19}$$

where $\mathbf{y}$ is the dual variable corresponding to the primary variable $\boldsymbol{x}$.

5) Subgradient: The subgradient of $f : \mathcal{H} \to \overline{\mathcal{R}}$ at point $\mathbf{x}$ is defined as

$$\partial f := \{\mathbf{p} \in \mathcal{H} | f(\mathbf{y}) \ge f(\mathbf{x}) + \langle \mathbf{p}, \mathbf{y} - \mathbf{x}\rangle, \forall \mathbf{y} \in \mathcal{H}\}. \tag{20}$$

6) Proximal Operator: The proximal operator of a convex function f is defined as

$$\mathbf{prox}_{\tau f}(\mathbf{y}) = \arg\min_{\mathbf{x}\in\mathcal{H}}\left\{f(\mathbf{x}) + \frac{1}{2\tau}\|\mathbf{x} - \mathbf{y}\|^2\right\}. \tag{21}$$

B. Model of the Communication Network

An undirected graph $\mathcal{G} = \{\mathcal{V}, \mathcal{E}\}$ is designed to describe the communication network between the multiple EHs, where each vertex $v_i \in \mathcal{V}$ denotes the ith EH and each edge $e_{ij} = (v_i, v_j) \in \mathcal{E}$ denotes a communication link with a positive weight ω_{ij} between the vertex v_i and the vertex v_j. In addition, $\mathcal{N}_i = \{j | e_{ij} \in \mathcal{E}\}$ is used to denote all the neighbors of the ith EH. Furthermore, we consider that the weight matrix $\mathbf{W}$ of the communication network has the following requirements:

$$\text{(Positive-definiteness) } \mathbf{W}^{\mathbf{T}} = \mathbf{W} \text{ and } \mathbf{W} \succ \mathbf{0} \tag{22}$$

$$\text{(Stochasticity) } \mathbf{W1} = \mathbf{1} \text{ or } \mathbf{1}^{\mathbf{T}}\mathbf{W} = \mathbf{1}^{\mathbf{T}} \tag{23}$$

$$\textit{(Connectivity) } \eta_{\mathbf{0}} := \rho\left(\mathbf{W} - \frac{\mathbf{11}^{\mathbf{T}}}{m}\right) < \mathbf{1}. \tag{24}$$

Thus, $\text{null}(\mathbf{I} - \mathbf{W}) = \text{span}\{\mathbf{1}\}$ can be derived from the above requirements. And the further selection of the weight matrix $\mathbf{W}$ is detailed in [36].

C. Dual Optimal Consensus Model and Feasibility

The global Lagrange function for (14) and (15) is cast as

$$L(\boldsymbol{\lambda}, \mathbf{x}) := \sum_{i=1}^{m} L_i(\boldsymbol{\lambda}, \mathbf{x}_i) \tag{25}$$

where $\boldsymbol{\lambda} = [0, 0, 0, \lambda_1, \lambda_2, \lambda_3]^T$ is the dual variables and the local Lagrange function for the ith EH is

$$L_i(\boldsymbol{\lambda}, \mathbf{x}_i) = f_i^0(\mathbf{x}_i) - \boldsymbol{\lambda}^T\mathbf{x}_i. \tag{26}$$

Then, the dual problem for the ith EH is

$$D_i(\boldsymbol{\lambda}) = \inf_{\mathbf{x}_i} L_i(\boldsymbol{\lambda}, \mathbf{x}_i) = \left(f_i^0\right)^*(\boldsymbol{\lambda}) \tag{27}$$

where $(f_i^0)^*$ the convex conjugate of f_i^0 and can be gathered together to formulate a popular distributed optimization problem as

$$\min_{\lambda\in\mathcal{H}} \sum_{i=1}^{m} D_i(\boldsymbol{\lambda}) = \sum_{i=1}^{m}\left(f_i^0\right)^*(\boldsymbol{\lambda}). \tag{28}$$

Note that the dual variables are shared among all the EHs. To realize a distributed way, a reformulation can be performed with the duplicated dual variables and one constraint is added to guarantee the equivalence among the duplicated variables. This therefore gives a decomposable problem, such that

$$\min_{\mathbf{y}\in\mathcal{H}} f^*(\mathbf{y}) = \sum_{i=1}^{m}\left(f_i^0\right)^*(\mathbf{y}_i) \tag{29}$$

$$\text{s.t. } \mathbf{y}^1 = \mathbf{y}^2 = \mathbf{y}^3 = \mathbf{0} \tag{30}$$

$$\mathbf{y}_i^4 = \mathbf{y}_j^4, \mathbf{y}_i^5 = \mathbf{y}_j^5, \mathbf{y}_i^6 = \mathbf{y}_j^6 \quad \forall i, j \in \mathcal{V} \tag{31}$$

where the duplicated variable $\mathbf{y}_i$ equals λ. Resorting to [36], since it holds for $\text{null}(\mathbf{I} - \mathbf{W}) = \text{span}\{1\}$ from (22)–(24), it can be known that, if the communication network topology is connected, problem (29)–(31) is the same as the following OCP:

$$\min_{\mathbf{y}\in\mathcal{H}} f^*(\mathbf{y}) = \sum_{i=1}^{m}(f_i + t_i)^*(\mathbf{y}_i) \tag{32}$$

$$\text{s.t.}\ \mathbf{y}^1 = \mathbf{y}^2 = \mathbf{y}^3 = \mathbf{0} \tag{33}$$

$$(\mathbf{I}-\mathbf{W})\mathbf{y}^4 = \mathbf{0}, (\mathbf{I}-\mathbf{W})\mathbf{y}^5 = \mathbf{0}, (\mathbf{I}-\mathbf{W})\mathbf{y}^6 = \mathbf{0} \quad \forall i, j \in \mathcal{V}. \tag{34}$$

In a compact form, the OCP can be rewritten as

$$\min_{\mathbf{y}\in\mathcal{H}} f^*(\mathbf{y}) = \sum_{i=1}^{m}(f_i + t_i)^*(\mathbf{y}_i) \tag{35}$$

$$\text{s.t.}\ (\mathbf{I}-\mathbf{T})\mathbf{y} = \mathbf{0} \quad \forall i, j \in \mathcal{V} \tag{36}$$

where $\mathbf{T}$ is defined as the augmented weight matrix which is structured as follows:

$$\mathbf{T}_{6m\times 6m} = \begin{bmatrix} \alpha\mathbf{I}_3 & \mathbf{O}_{3\times3} & \cdots & \mathbf{O}_{3\times3} & \mathbf{O}_{3\times3} \\ \mathbf{O}_{3\times3} & \omega_{11}\mathbf{I}_3 & \cdots & \mathbf{O}_{3\times3} & \omega_{1m}\mathbf{I}_3 \\ \vdots & \vdots & \ddots & \vdots & \vdots \\ \mathbf{O}_{3\times3} & \mathbf{O}_{3\times3} & \cdots & \alpha\mathbf{I}_3 & \mathbf{O}_{3\times3} \\ \mathbf{O}_{3\times3} & \omega_{m1}\mathbf{I}_3 & \cdots & \mathbf{O}_{3\times3} & \omega_{mm}\mathbf{I}_3 \end{bmatrix} \tag{37}$$

where $\alpha \in (0, 1)$ is a real number.

Finally, the original problem (OEP) in (14) and (15) and the dual problem (OCP) in (35) and (36) constitute the *primal–dual problem*, called as OCEP problem. Accordingly, the KKT conditions of the OCEP problem can be presented as

$$(\text{Primal Feasibility} - \text{OEP}) \quad \mathbf{B}^T\mathbf{x}^* = \mathbf{0} \tag{38}$$

$$(\text{Dual Feasibility} - \text{OCP}) \quad (\mathbf{I}-\mathbf{T})\mathbf{y}^* = \mathbf{0} \tag{39}$$

$$(\text{Lagrangian Optimality}) \quad \mathbf{y}^* - \nabla f(\mathbf{x}^*) \in \partial t(\mathbf{x}^*). \tag{40}$$

D. Distributed Algorithm

It should be noted that the essential aim of this article is to solve the primal OEP problem in a distributed way. To reach this goal, we tend to solve the dual OCP problem alternatively in a distributed way. Resorting to our previous works [36] and [39], we can obtain the following algorithm:

$$\mathbf{y}_{k+1} = \mathbf{y}_k + \tau(2\mathbf{x}_k - \mathbf{x}_{k-1} - \mathbf{z}_k) \tag{41}$$

$$\mathbf{x}_{k+1} = \mathbf{x}_k - \frac{1}{\tau}(\mathbf{I}-\mathbf{T})\mathbf{y}_{k+1} \tag{42}$$

$$\mathbf{z}_{k+1} = \mathbf{prox}_{\gamma t}(\mathbf{z}_k - \gamma)\nabla f\big(\mathbf{z}_k(-2\mathbf{y}_{k+1} + \mathbf{y}_k)\big) \tag{43}$$

where $\mathbf{z}_k$ is the auxiliary variable which is embedded in (41) and updated by using the latest information of y_{k+1}. From step 4 in the algorithm, it is obvious that each EH only needs its local information such that the algorithm can be performed in a distributed way. Note, the primal feasibility always holds for the OEP during the iteration, if the initial value is proper. This is a very useful property in the practical engineering application. For the optimal dispatch of an IES, the energy balance constraint is critical to the secure operation. From a physical viewpoint, the operators usually expect to fast find a feasible solution and then gradually improve the feasible solution toward the optimal solution. Most importantly, the improvement at each step will strictly guarantee the energy balance; otherwise, the energy system will lose the steady-state point.

In addition, the convergence criteria of the proposed algorithm should be defined as: the KKT condition holds, or the maximum number of iterations is achieved. Finally, the distributed algorithm can be summarized as in Algorithm 1, where $(\mathbf{x}_{i,k}, \mathbf{y}_{i,k}, \mathbf{z}_{i,k})$ are the ith components of the vectors $(\mathbf{x}_k, \mathbf{y}_k, \mathbf{z}_k)$ in (41)–(43); taking (37) in (42) will give the step 4.

Algorithm 1 DD-Based Distributed Algorithm

1. **Initialization**: Let $\mathbf{x}_{i,0} = 0, \forall i \in \mathcal{V}$ such that $\mathbf{B}^{\mathrm{T}}\mathbf{x}_0 = \mathbf{0}$, and choose any value for $\mathbf{y}_0, \mathbf{z}_0, \mathbf{x}_{-1}$.
2. **While** the algorithm is not converged
3. **Dual Update**: For $\forall i \in \mathcal{V}$, do
$$\mathbf{y}_{i,k+1} = \mathbf{y}_{i,k} + \tau(2\mathbf{x}_{i,k} - \mathbf{x}_{i,k-1} - \mathbf{z}_{i,k}),$$
4. **Primal Update**: For $\forall i \in \mathcal{V}$,
$$\begin{aligned}(x_{6i-5}, x_{6i-4}, x_{6i-3})^T_{k+1} &= (x_{6i-5}, x_{6i-4}, x_{6i-3})^T_k \\ &\quad - \frac{1}{\tau}(1-\alpha)(y_{6i-5}, y_{6i-4}, y_{6i-3})^T_{k+1}, \\ (x_{6i-2}, x_{6i-1}, x_{6i})^T_{k+1} &= (x_{6i-2}, x_{6i-1}, x_{6i})^T_k \\ &\quad - \frac{1}{\tau}\sum_{j\in\mathcal{N}_i}\omega_{ij}\Big((y_{6i-5}, y_{6i-4}, y_{6i-3})^T_{k+1} - (y_{6j-5}, y_{6j-4}, y_{6j-3})^T_{k+1}\Big),\end{aligned} \tag{44}$$
5. **Update of Auxiliary Variable**: For $\forall i \in \mathcal{V}$, do
$$\mathbf{z}_{i,k+1} = \mathbf{prox}_{\gamma t_i}(\mathbf{z}_{i,k} - \gamma(\nabla f_i(\mathbf{z}_{i,k}) - 2\mathbf{y}_{i,k+1} + \mathbf{y}_{i,k})).$$
6. Set $k \to k+1$ and go to the **Step 3**
7. **End**

IV. Linear Convergence Analysis

The proposed DD-based distributed algorithm has a linear convergence rate for the optimization models with separable convex quadratic objective functions. To theoretically show the convergence performance of the proposed method, we will at first give some basic lemmas and theorems.

A. Basic Lemmas

At the beginning, several lemmas are proved for the later convergence analysis.

Lemma 1: According to the requirements of weight matrix, the augmented weight matrix $\mathbf{T}$ has the following properties:

$$(\text{Positive} - \text{definiteness}) \quad \mathbf{T}^{\mathbf{T}} = \mathbf{T} \text{ and } \mathbf{T} > \mathbf{0} \tag{45}$$

$$(\text{Stochasticity}) \quad \mathbf{TB} = \mathbf{B} \text{ or } \mathbf{B}^{\mathbf{T}}\mathbf{T} = \mathbf{B}^{\mathbf{T}} \tag{46}$$

$$(\text{Connectivity}) \quad \eta := \rho\left(\mathbf{T} - \frac{BB^{\mathbf{T}}}{m}\right) < 1. \tag{47}$$

Proof: We consider that the characteristic polynomial of the $\mathbf{T}$ is $g_{\mathbf{T}}(\xi)$ and the characteristic polynomial of the $\mathbf{W}$ is $g_{\mathbf{W}}(\xi)$. The relationship between $g_{\mathbf{T}}(\xi)$ and $g_{\mathbf{W}}(\xi)$ can be derived as

$$g_{\mathbf{T}}(\xi) = |\xi\mathbf{I} - \mathbf{T}| = \begin{vmatrix} (\xi-\alpha)\mathbf{I}_3 & \mathbf{O}_{3\times3} & \cdots & \mathbf{O}_{3\times3} & \mathbf{O}_{3\times3} \\ \mathbf{O}_{3\times3} & (\xi-\omega_{11})\mathbf{I}_3 & \cdots & \mathbf{O}_{3\times3} & -\omega_{1m}\mathbf{I}_3 \\ \vdots & \vdots & \ddots & \vdots & \vdots \\ \mathbf{O}_{3\times3} & \mathbf{O}_{3\times3} & \cdots & (\xi-\alpha)\mathbf{I}_3 & \mathbf{O}_{3\times3} \\ \mathbf{O}_{3\times3} & -\omega_{m1}\mathbf{I}_3 & \cdots & \mathbf{O}_{3\times3} & (\xi-\omega_{mm})\mathbf{I}_3 \end{vmatrix}.$$

This article has been accepted for inclusion in a future issue of this journal. Content is final as presented, with the exception of pagination.

After the row and column transformations, the above determinant can be rewritten by

$$
\begin{aligned}
g_{\mathbf{T}}(\xi) &= \begin{vmatrix}
(\xi-\alpha)\mathbf{I}_3 &&&&&&& \\
& (\xi-\alpha)\mathbf{I}_3 &&&&&& \\
&& \ddots &&&&& \\
&&& (\xi-\alpha)\mathbf{I}_3 &&&& \\
&&&& (\xi-\omega_{11})\mathbf{I}_3 & -\omega_{12}\mathbf{I}_3 & \cdots & -\omega_{1m}\mathbf{I}_3 \\
&&&& -\omega_{21}\mathbf{I}_3 & (\xi-\omega_{22})\mathbf{I}_3 & \cdots & -\omega_{2m}\mathbf{I}_3 \\
&&&& \vdots & \vdots & \ddots & \vdots \\
&&&& -\omega_{1m}\mathbf{I}_3 & -\omega_{12}\mathbf{I}_3 & \cdots & (\xi-\omega_{1m})\mathbf{I}_3
\end{vmatrix} \\
&= (\xi-\alpha)^{3m} \begin{vmatrix}
(\xi-\omega_{11})\mathbf{I}_3 & -\omega_{12}\mathbf{I}_3 & \cdots & -\omega_{1m}\mathbf{I}_3 \\
-\omega_{21}\mathbf{I}_3 & (\xi-\omega_{22})\mathbf{I}_3 & \cdots & -\omega_{2m}\mathbf{I}_3 \\
\vdots & \vdots & \ddots & \vdots \\
-\omega_{1m}\mathbf{I}_3 & -\omega_{12}\mathbf{I}_3 & \cdots & (\xi-\omega_{1m})\mathbf{I}_3
\end{vmatrix}.
\end{aligned} \tag{48}
$$

For convenience, we define

$$
K(\xi) = \begin{vmatrix}
(\xi-\omega_{11})\mathbf{I}_3 & -\omega_{12}\mathbf{I}_3 & \cdots & -\omega_{1m}\mathbf{I}_3 \\
-\omega_{21}\mathbf{I}_3 & (\xi-\omega_{22})\mathbf{I}_3 & \cdots & -\omega_{2m}\mathbf{I}_3 \\
\vdots & \vdots & \ddots & \vdots \\
-\omega_{1m}\mathbf{I}_3 & -\omega_{12}\mathbf{I}_3 & \cdots & (\xi-\omega_{1m})\mathbf{I}_3
\end{vmatrix}. \tag{49}
$$

After the expansion and row-column transformation of $K(\xi)$, we have (50), as shown at the bottom of the page.

Furthermore, we have the relationship

$$
g_{\mathbf{T}}(\xi) = (\xi-\alpha)^{3m}(g_W(\xi))^3. \tag{51}
$$

From the above equation, we can know that the eigenvalues of $\mathbf{T}$ are determined by

$$
\xi(\mathbf{T}) = \{\alpha, \xi(\mathbf{W})\}. \tag{52}
$$

It is known that $\mathbf{W}$ has a simple eigenvalue one with others belonging to (0, 1). Since $\alpha \in (0, 1)$, we can know that $\mathbf{T}$ has $3m$ simple eigenvalue ones but others belong to (0, 1). Therefore, $\mathbf{T}$ is positive definite.

Moreover, according to (22), we have $\omega_{ij} = \omega_{ji}, \forall i, j \in \mathcal{V}$. Then, the structure of $\mathbf{T}$ is also symmetric, such that $(T^T = T)$. Thus, the condition (45) holds.

Furthermore, we divide $\mathbf{B}$ into blocks by the column as

$$
\mathbf{B} = \left[\mathbf{0}, \mathbf{0}, \mathbf{0}, \boldsymbol{\beta}_1, \boldsymbol{\beta}_2, \boldsymbol{\beta}_3\right] \tag{53}
$$

with

$$
\boldsymbol{\beta}_1 = [0, 0, 0, 1, 0, 0, \ldots, 0, 0, 0, 1, 0, 0]^T \tag{54}
$$
$$
\boldsymbol{\beta}_2 = [0, 0, 0, 0, 1, 0, \ldots, 0, 0, 0, 0, 1, 0]^T \tag{55}
$$
$$
\boldsymbol{\beta}_3 = [0, 0, 0, 0, 0, 1, \ldots, 0, 0, 0, 0, 0, 1]^T. \tag{56}
$$

Thus, if we want to prove $\mathbf{TB} = \mathbf{B}$, it is equivalent to prove $\mathbf{T}[\boldsymbol{\beta}_1, \boldsymbol{\beta}_2, \boldsymbol{\beta}_3] = [\boldsymbol{\beta}_1, \boldsymbol{\beta}_2, \boldsymbol{\beta}_3]$.

From (23), it is observed that $\mathbf{W1} = \mathbf{1}$, which can be expanded into

$$
\begin{bmatrix}
\omega_{11} & \omega_{12} & \cdots & \omega_{1m} \\
\omega_{21} & \omega_{21} & \cdots & \omega_{2m} \\
\vdots & \vdots & \ddots & \vdots \\
\omega_{m1} & \omega_{m2} & \cdots & \omega_{mm}
\end{bmatrix}
\begin{bmatrix} 1 \\ 1 \\ \vdots \\ 1 \end{bmatrix}
=
\begin{bmatrix} 1 \\ 1 \\ \vdots \\ 1 \end{bmatrix}. \tag{57}
$$

After adding some zero elements on the above $\mathbf{1}$ vector and changing $\mathbf{W}$, we have

$$
\begin{bmatrix}
\alpha &&&&&&&&&&& \\
& \alpha &&&&&&&&&& \\
&& \alpha &&&&&&&&& \\
&&& \omega_{11} &&& \cdots &&& \omega_{1m} && \\
&&&& \omega_{11} &&& \cdots &&& \omega_{1m} & \\
&&&&& \omega_{11} &&& \cdots &&& \omega_{1m} \\
&&& \vdots &&& \ddots &&&& \vdots & \\
&&&&&& \alpha &&&&& \\
&&&&&&& \alpha &&&& \\
&&&&&&&& \alpha &&& \\
&&& \omega_{m1} &&& \cdots &&& \omega_{mm} && \\
&&&& \omega_{m1} &&& \cdots &&& \omega_{mm} & \\
&&&&& \omega_{m1} &&& \cdots &&& \omega_{mm}
\end{bmatrix}
$$

$$
\begin{aligned}
K(\xi) &= \begin{vmatrix}
\begin{matrix}
\xi-\omega_{11} & -\omega_{12} & \cdots & -\omega_{1m} \\
-\omega_{21} & \xi-\omega_{22} & \cdots & -\omega_{2m} \\
\vdots & \vdots & \ddots & \vdots \\
-\omega_{1m} & -\omega_{12} & \cdots & \xi-\omega_{1m}
\end{matrix} && \\
& \begin{matrix}
\xi-\omega_{11} & -\omega_{12} & \cdots & -\omega_{1m} \\
-\omega_{21} & \xi-\omega_{22} & \cdots & -\omega_{2m} \\
\vdots & \vdots & \ddots & \vdots \\
-\omega_{1m} & -\omega_{12} & \cdots & \xi-\omega_{1m}
\end{matrix} & \\
&& \begin{matrix}
\xi-\omega_{11} & -\omega_{12} & \cdots & -\omega_{1m} \\
-\omega_{21} & \xi-\omega_{22} & \cdots & -\omega_{2m} \\
\vdots & \vdots & \ddots & \vdots \\
-\omega_{1m} & -\omega_{12} & \cdots & \xi-\omega_{1m}
\end{matrix}
\end{vmatrix} \\
&= \begin{vmatrix}
\xi\mathbf{I}-\mathbf{W} && \\
& \xi\mathbf{I}-\mathbf{W} & \\
&& \xi\mathbf{I}-\mathbf{W}
\end{vmatrix} = (g_{\mathbf{W}}(\xi))^3
\end{aligned} \tag{50}
$$

$$\times\begin{bmatrix}0\\0\\0\\1\\0\\0\\\vdots\\0\\0\\0\\1\\0\\0\end{bmatrix}=\begin{bmatrix}0\\0\\0\\1\\0\\0\\\vdots\\0\\0\\0\\1\\0\\0\end{bmatrix} \quad (58)$$

where $\mathbf{T}\boldsymbol{\beta}_1 = \boldsymbol{\beta}_1$.

Similarly, we have $\mathbf{T}[\boldsymbol{\beta}_1, \boldsymbol{\beta}_2, \boldsymbol{\beta}_3] = [\boldsymbol{\beta}_1, \boldsymbol{\beta}_2, \boldsymbol{\beta}_3]$, such that $\mathbf{TB} = \mathbf{B}$ is ensured. If we transpose both sides on $\mathbf{TB} = \mathbf{B}$ with $\mathbf{T}$ being symmetrical, it yields $\mathbf{B^T T} = \mathbf{B^T}$.

Let $\mathbf{W}^{(1)} = \mathbf{W} - (\mathbf{1}\mathbf{1}^T/m)$, then $\rho(\mathbf{W}^{(1)}) < 1$ from (24). Further

$$\begin{aligned}\mathbf{BB}^{\mathrm{T}} &= \begin{bmatrix} & & \mathbf{O}_{3\times 6m} & & \\ \mathbf{O}_{3\times3} & \mathbf{I}_{3\times3} & \cdots & \mathbf{O}_{3\times3} & \mathbf{I}_{3\times3}\end{bmatrix}^{\mathrm{T}} \\ &\quad\times\begin{bmatrix} & & \mathbf{O}_{3\times 6m} & & \\ \mathbf{O}_{3\times3} & \mathbf{I}_{3\times3} & \cdots & \mathbf{O}_{3\times3} & \mathbf{I}_{3\times3}\end{bmatrix} \\ &= \begin{bmatrix}\mathbf{O}_{3\times3} & \mathbf{O}_{3\times3} & \cdots & \mathbf{O}_{3\times3} & \mathbf{O}_{3\times3}\\ \mathbf{O}_{3\times3} & \mathbf{I}_{3\times3} & \cdots & \mathbf{I}_{3\times3} & \mathbf{O}_{3\times3}\\ \vdots & \vdots & \ddots & \vdots & \vdots\\ \mathbf{O}_{3\times3} & \mathbf{O}_{3\times3} & \cdots & \mathbf{O}_{3\times3} & \mathbf{O}_{3\times3}\\ \mathbf{O}_{3\times3} & \mathbf{I}_{3\times3} & \cdots & \mathbf{I}_{3\times3} & \mathbf{O}_{3\times3}\end{bmatrix}. \end{aligned} \quad (59)$$

Then, it attains

$$\begin{aligned}&\mathbf{T} - \frac{B B^{\mathbf{T}}}{m} \\ &= \begin{bmatrix}\alpha\mathbf{I}_3 & \mathbf{O}_{3\times3} & \cdots & \mathbf{O}_{3\times3} & \mathbf{O}_{3\times3}\\ \mathbf{O}_{3\times3} & \left(\omega_{11} - \frac{1}{m}\right)\mathbf{I}_3 & \cdots & \mathbf{O}_{3\times3} & \left(\omega_{1m} - \frac{1}{m}\right)\mathbf{I}_3\\ \vdots & \vdots & \ddots & \vdots & \vdots\\ \mathbf{O}_{3\times3} & \mathbf{O}_{3\times3} & \cdots & \alpha\mathbf{I}_3 & \mathbf{O}_{3\times3}\\ \mathbf{O}_{3\times3} & \left(\omega_{m1} - \frac{1}{m}\right)\mathbf{I}_3 & \cdots & \mathbf{O}_{3\times3} & \left(\omega_{mm} - \frac{1}{m}\right)\mathbf{I}_3\end{bmatrix}.\end{aligned} \quad (60)$$

Let $\mathbf{T}^{(1)} = \mathbf{T} - (\mathbf{BB}^T/m)$ and consider the determinant of $\mathbf{T}^{(1)}$

$$\begin{aligned}&g_{\mathbf{T}^{(1)}}(\xi) \\ &= \left|\xi\mathbf{I} - \mathbf{T}^{(1)}\right| \\ &= \begin{bmatrix}(\xi-\alpha)\mathbf{I}_3 & \mathbf{O}_{3\times3} & \cdots & \mathbf{O}_{3\times3} & \mathbf{O}_{3\times3}\\ \mathbf{O}_{3\times3} & \left(\xi - \omega_{11} + \frac{1}{m}\right)\mathbf{I}_3 & \cdots & \mathbf{O}_{3\times3} & \left(1 - \omega_{1m} + \frac{1}{m}\right)\mathbf{I}_3\\ \vdots & \vdots & \ddots & \vdots & \vdots\\ \mathbf{O}_{3\times3} & \mathbf{O}_{3\times3} & \cdots & (\xi-\alpha)\mathbf{I}_3 & \mathbf{O}_{3\times3}\\ \mathbf{O}_{3\times3} & \left(1 - \omega_{m1} + \frac{1}{m}\right)\mathbf{I}_3 & \cdots & \mathbf{O}_{3\times3} & \left(\xi - \omega_{mm} + \frac{1}{m}\right)\mathbf{I}_3\end{bmatrix}.\end{aligned} \quad (61)$$

With respect to (48)–(51), the row–column transformation to $g_{\mathbf{T}}(\xi)$ gives

$$g_{\mathbf{T}^{(1)}} = (\xi-\alpha)^{3m}\left(g_{\mathbf{W}^{(1)}}(\xi)\right)^3. \quad (62)$$

Thus, we have

$$\xi\left(\mathbf{T}^{(1)}\right) = \left\{\alpha, \xi\left(\mathbf{W}^{(1)}\right)\right\}. \quad (63)$$

Therefore, (24) and $\alpha \in (0, 1)$, it is known that $\rho(\mathbf{T}^{(1)}) < 1$, that is, $\rho(\mathbf{T} - (\mathbf{BB^T}/m)) < 1$. ∎

Lemma 2 (Feasibility): Given the initialization value $\mathbf{x}_0$, $\mathbf{B}^T\mathbf{x}_k = 0\ \forall k \geq 0$ is guaranteed if $\mathbf{B}^T\mathbf{x}_0 = \mathbf{0}$ and *assumptions of Lemma 1* are satisfied.

Proof: Multiplying $\mathbf{B}^T$ to both sides of (42) offers

$$\begin{aligned}\mathbf{B}^T\mathbf{x}_{k+1} &= \mathbf{B}^T\mathbf{x}_k - \frac{1}{\tau}\mathbf{B}^T(\mathbf{I}-\mathbf{T})\mathbf{y}_{k+i} \\ &= \mathbf{B}^T\mathbf{x}_k - \frac{1}{\tau}(\mathbf{B}^T - \mathbf{B}^T\mathbf{T})\mathbf{y}_{k+i}.\end{aligned} \quad (64)$$

From (46), it is known from Lemma 1 that $\mathbf{B^T T} = \mathbf{B^T}$ holds, which gives the following equation:

$$\mathbf{B}^T\mathbf{x}_{k+1} = \mathbf{B}^T\mathbf{x}_k - \frac{1}{\tau}\mathbf{B}^T(\mathbf{B}^T - \mathbf{B}^T)\mathbf{y}_{k+i} = \mathbf{B}^T\mathbf{x}_k. \quad (65)$$

Thus, we will know that $\mathbf{B}^T\mathbf{x}_k = \mathbf{0}\ \forall k \geq 0$ is true by mathematical induction if $\mathbf{B}^T\mathbf{x}_0 = \mathbf{0}$. ∎

Lemma 3 (Bijective Transformation): Let $\mathbf{P} = \mathbf{I} - \mathbf{T}$ such that $\mathrm{null}(\mathbf{P}) = \mathrm{span}\{\boldsymbol{\beta}_1, \boldsymbol{\beta}_2, \boldsymbol{\beta}_3\}$, where $\mathbf{T}$ satisfies Lemma 1. For each $x \in \mathrm{span}^{\perp}\{\boldsymbol{\beta}_1, \boldsymbol{\beta}_2, \boldsymbol{\beta}_3\}$ and $x' \in \mathrm{span}^{\perp}\{\boldsymbol{\beta}_1, \boldsymbol{\beta}_2, \boldsymbol{\beta}_3\}$ is uniquely determined by $x = Px'$ and vice versa. This means that there exists a bijective transformation $\mathbf{P}$ between $x \in \mathrm{span}^{\perp}\{\boldsymbol{\beta}_1, \boldsymbol{\beta}_2, \boldsymbol{\beta}_3\}$ and $x' \in \mathrm{span}^{\perp}\{\boldsymbol{\beta}_1, \boldsymbol{\beta}_2, \boldsymbol{\beta}_3\}$.

Proof: Due to $\mathrm{null}(\mathbf{P}) = \mathrm{span}\{\boldsymbol{\beta}_1, \boldsymbol{\beta}_2, \boldsymbol{\beta}_3\}$, we have

$$\mathbf{P}\left[\boldsymbol{\beta}_1, \boldsymbol{\beta}_2, \boldsymbol{\beta}_3\right] = \mathbf{O} \quad (66)$$

$$r(P) + r\left(\left[\boldsymbol{\beta}_1, \boldsymbol{\beta}_2, \boldsymbol{\beta}_3\right]\right) = 6m. \quad (67)$$

From (54)–(56), we know $r([\boldsymbol{\beta}_1, \boldsymbol{\beta}_2, \boldsymbol{\beta}_3]) = 3$, giving

$$r(\mathbf{P}) = 6m - 3. \quad (68)$$

Transposing both sides on (66) leads to

$$\left[\boldsymbol{\beta}_1, \boldsymbol{\beta}_2, \boldsymbol{\beta}_3\right]^T\mathbf{P}^T = \mathbf{O}. \quad (69)$$

From (45), we know $\mathbf{P} = \mathbf{P}^T$ such that

$$\left[\boldsymbol{\beta}_1, \boldsymbol{\beta}_2, \boldsymbol{\beta}_3\right]^T P = O. \quad (70)$$

Note that $\mathbf{x} \in \mathrm{span}^{\perp}\{\boldsymbol{\beta}_1, \boldsymbol{\beta}_2, \boldsymbol{\beta}_3\}$, which results in

$$\left[\boldsymbol{\beta}_1, \boldsymbol{\beta}_2, \boldsymbol{\beta}_3\right]^T\mathbf{x} = \mathbf{0}. \quad (71)$$

Based on (68) and (70), divide $\mathbf{P}$ into columns as

$$\mathbf{P} = \left[\mathbf{p}_1, \mathbf{p}_2, \ldots, \mathbf{p}_{6m}\right]. \quad (72)$$

This leads to $\mathrm{null}([\boldsymbol{\beta}_1, \boldsymbol{\beta}_2, \boldsymbol{\beta}_3]) = \mathrm{span}\{\mathbf{p}_1, \mathbf{p}_2, \ldots, \mathbf{p}_{6m}\}$. Thus, from (71), we know that

$$r(\mathbf{P}, \mathbf{x}) = 6m - 3. \quad (73)$$

Considering both (68) and (73), there exists $\mathbf{x}'$ such that $\mathbf{x} = \mathbf{P}\mathbf{x}'$.

If $\mathbf{x}' \in \mathrm{span}^{\perp}\{\boldsymbol{\beta}_1, \boldsymbol{\beta}_2, \boldsymbol{\beta}_3\}$ such that $[\boldsymbol{\beta}_1, \boldsymbol{\beta}_2, \boldsymbol{\beta}_3]^T\mathbf{x}' = \mathbf{O}$, it gives

$$\left[P, \boldsymbol{\beta}_1, \boldsymbol{\beta}_2, \boldsymbol{\beta}_3\right]^T\mathbf{x}' = \left[\mathbf{x}^T, 0, 0, 0\right]^T. \quad (74)$$

From (66) and (72), we know $r([\mathbf{P}, \boldsymbol{\beta}_1, \boldsymbol{\beta}_2, \boldsymbol{\beta}_3]) = 6m$, thus, $\mathbf{x}'$ is unique and the reverse transformation is similar. ■

Lemma 4: $\mathbf{Q} = \mathbf{I} - (\mathbf{T} - (\mathbf{B}^T\mathbf{B}/m))$ is positive definite.

According to (47) that $\rho(\mathbf{T}-(\mathbf{B}\mathbf{B}^{\mathbf{T}}/m)) < 1$, we can directly deduce that $\xi(\mathbf{Q}) > 0$. Hence, Lemma 4 holds.

B. Linear Convergence Rate Analysis

From our previous work, we have the following theorem.

Theorem [39]: For given $\gamma < [(\xi_{\min}\mathbf{W})/(4(L_f + l_f)\xi_{\min}(\mathbf{W}) + 5\tau)]$ and $\tau < [L_f l_f/(L_f + l_f)]$, the sequence $\{\{\mathbf{x}_k, \mathbf{y}_k\}\}_{k\geq 0}$ generated by the DD converges linearly to the optimum $[\mathbf{x}^*, \mathbf{y}^*]$, such that

$$\left\|[\mathbf{x}_{k+1}, \mathbf{y}_{k+1}] - [\mathbf{x}^*, \mathbf{y}^*]\right\|^2_{\mathbf{H}'} \leq (1-\delta)\left\|[\mathbf{x}_k, \mathbf{y}_k] - [\mathbf{x}^*, \mathbf{y}^*]\right\|^2_{\mathbf{H}'} \tag{75}$$

where

$$\mathbf{H}' = \begin{bmatrix} \gamma\tau\mathbf{I} + \mathbf{W} & \mathbf{O} & -\tau\mathbf{I} \\ \mathbf{O} & \tau^2(\gamma\tau\mathbf{I} + \mathbf{Q}^{-1}) & \mathbf{O} \\ -\tau\mathbf{I} & \mathbf{O} & \frac{\tau}{\gamma}\mathbf{I} \end{bmatrix}$$

and $\delta = \min\{[\gamma\tau/(4\gamma\tau + 2)],\ \gamma([L_f l_f/(L_f + l_f)] - \tau),\ [(\gamma\tau(1-\eta))/(2-\eta)]\}$. If the following conditions are satisfied.

1) The given $\mathbf{Q}$ satisfies positive definiteness, stochasticity, and connectivity.
2) The function t_i is closed and convex. The function $f_i(\mathbf{x})$ is $l_{f_i}-$strongly convex and $L_{f_i}-$smooth, which gives
$$\begin{aligned} l_{f_i}\left\|\mathbf{x}_i^{\cdot} - \mathbf{x}_i\right\| &\leq \left\|\nabla f_i(\mathbf{x}_i^{\cdot}) - \nabla f_i(\mathbf{x}_i)\right\| \\ &\leq L_{f_i}\left\|\mathbf{x}_i^{\cdot} - \mathbf{x}_i\right\|\ \forall \mathbf{x}_i, \mathbf{x}_i^{\cdot} \in \mathcal{H}. \end{aligned} \tag{76}$$
3) The bijective transformation is satisfied in the disagreement space and the primary feasibility always holds for the decomposition method.

According to Lemmas 1 and 4, we can know that $\mathbf{T}$ satisfies positive definiteness, stochasticity, and connectivity. Therefore, the condition 1) holds for the proposed DD method with the weight matrix $\mathbf{T}$.

For the model (1)–(8), the objective function is the summation of several separable convex quadratic functions and, moreover, for each $i \in \mathcal{V}$, the function $t_i = 0$. As a result, $f(\mathbf{x})$ is written as $f(\mathbf{x}) = \sum_{i=1}^m f_i(\mathbf{x}_i) = \sum_{i=1}^m (\mathbf{a}_i\mathbf{x}_i^2 + \mathbf{b}_i\mathbf{x}_i + \mathbf{c}_i)$, where $\mathbf{a}_i > 0$. This gives the following equations

$$\left\|\nabla f_i(\mathbf{x}_i^{\cdot}) - \nabla f_i(\mathbf{x}_i)\right\| = 2\mathbf{a}_i\left\|\mathbf{x}_i^{\cdot} - \mathbf{x}_i\right\|, \forall \mathbf{x}_i, \mathbf{x}_i^{\cdot} \in \mathcal{H}. \tag{77}$$

Hence, it is easy to find that the $l_{f_i}-$strongly convex, differentiable and $L_{f_i} -$ smoothare satisfied. Moreover, we have $l_{f_i} = L_{f_i} = 2\mathbf{a}_i$. Furthermore, $f(\mathbf{x})$ has $L_f -$ smooth gradient with $L_f = \max\{2\mathbf{a}_i\}$ and is l_f-strongly convex with $l_f = \max\{2\mathbf{a}_i\}$. This shows that the condition 1) holds for the proposed DD method.

Finally, Lemma 2 shows that the bijective transformation of the weight matrix $\mathbf{T}$ is satisfied in the disagreement space; Lemma 3 gives the fact that the primary feasibility always holds for the decomposition method. Therefore, the condition 3) holds for the proposed DD method with the weight matrix $\mathbf{T}$.

Resorting to theorem in [39], the proposed DD method with the weight matrix $\mathbf{T}$ has a linear convergence rate to the optimal solution. In particular, we can derive from the aforementioned analysis that

$$\xi_{\min}(\mathbf{T}) = \min\{\alpha, \xi_{\min}(\mathbf{W})\}. \tag{78}$$

Furthermore, we have

$$\gamma < \frac{\min\{\alpha, \xi_{\min}(\mathbf{W})\}}{16\max\{\mathbf{a}_i\}\min\{\alpha, \xi_{\min}(\mathbf{W})\} + 5\tau}, \tau < \max\{\mathbf{a}_i\}. \tag{79}$$

V. Simulation Results

A. Data Collections

In this section, an m-IES with four EHs is designed for the proposed DD (and the energy output limits) method and each EH will purchase the energy from the external system to serve the total load demands. It should be noted that the topology of the communication networks and the energy transformation matrix of EHs may affect the convergence of the distributed algorithm. However, the energy transformation matrices are the prior parameters that are determined by the physical devices (e.g., energy conversion efficiency) and cannot be arbitrarily changed. In this article, according to [7], [41], and [42], we consider that 1 km^{3}natural gas burns to produce 32 GJ of energy and 1 MWh equals 3.6 GJ. Taking into account the loss ($\eta_{\text{loss}} \approx 0.9$) in the energy conversion process and 20% electricity or thermal energy is used for heating, the coefficient of electricity to heat is $\eta_{GH} = 20\% \times \eta_{\text{loss}} \times 32$ GJ $= 5.76$, and the coefficient of natural gas to heat is $\eta_{PH} = 20\% \times \eta_{\text{loss}} \times 3.6 = 0.65$. Therefore, the prior matrices $\mathbf{A}_i$ of the four EHs are considered the same as $\begin{bmatrix} 0.8 & 0 & 0 \\ 0.65 & 1 & 5.76 \\ 0 & 0 & 0.8 \end{bmatrix}$ and the and the corresponding energy output limits of each EH are shown in Table II. In contrast, the communication topology can be designed according to the practical engineering requirements. In order to analyze the impact of different communication topologies on the convergence performance, three different topologies are depicted in Fig. 2, where the node is the EH and the line denotes the communication link. Here, it should be noted that the total energy load demand (including electricity, heat, and gas) can be given as $P_L = 100.00$ MW, $H_L = 153.25$ GJ/h, and $G_L = 10.00$ km^3/h. The cost function can be expressed as a quadratic function by (9). Herein, $(a_i, b_i, c_i, d_i, e_i, f_i)$ are coefficients of the ith EH. In the practical engineering, the heat energy cannot be transferred in a long distance which instead should be self-sufficient in a local area. Therefore, we consider that the EHs do not purchase the heat energy from the external area. That means, $c_i = d_i = 0$ and $H_i^{\text{in}} = 0$. The other cost coefficients can be available in Table II. Besides, ADMM in [32] is employed to compare the proposed DD-based distributed algorithm. Meanwhile, the centralized optimal solution of the optimization model is directly solved by use of the GUROBI commercial optimization solver as the benchmark.

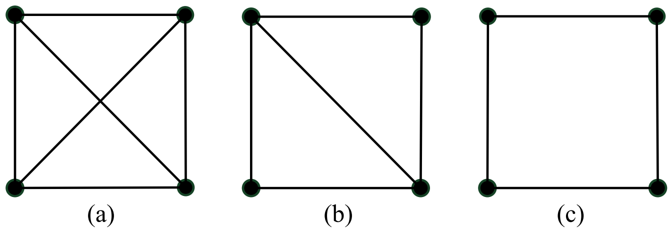

Fig. 2. Topology of the communication network. (a) Topology 1. (b) Topology 2. (c) Topology 3.

TABLE I
COST COEFFICIENTS OF THE EHs

EHs	a_i (¥/(MWh)^2)	b_i (¥/MWh)	e_i (k/(km^3)^2)	f_i (¥/km^3)
1	1	500	2	1500
2	1	450	2	1400
3	1	400	2	1500
4	0.8	350	1	1200

TABLE II
ENERGY OUTPUT LIMITS OF EHs

Case	Electricity Output Limits (MW)	Heat Ouput Limits (GJ/h)	Gas Ouput Limits (km^3/h)
A	[0, 2.00]	[0, 12.00]	[0, 1.50]
B	[0, 19.00]	[0, 50.00]	[0, 5.00]
C	[0, 40.00]	[0, 43.00]	[0, 1.50]
D	[0, 40.00]	[0, 50.00]	[0, 2.50]

TABLE III
ENERGY TRANSFORMATION BY EHs

EHs	Input Energy		Output Energy	
1	P_i^{in} (MW)	2.3189	P_i^{out} (MW)	1.8552
	H_i^{in} (GJ/h)	0.0000	H_i^{out} (GJ/h)	11.12887
	G_i^{in} (km^3/h)	1.6704	G_i^{out} (km^3/h)	1.3363
2	P_i^{in} (MW)	22.6811	P_i^{out} (MW)	18.1449
	H_i^{in} (GJ/h)	0.0000	H_i^{out} (GJ/h)	50.0000
	G_i^{in} (km^3/h)	6.1211	G_i^{out} (km^3/h)	4.8969
3	P_i^{in} (MW)	50.0000	P_i^{out} (MW)	40.0000
	H_i^{in} (GJ/h)	0.0000	H_i^{out} (GJ/h)	42.1213
	G_i^{in} (km^3/h)	1.6704	G_i^{out} (km^3/h)	1.3363
4	P_i^{in} (MW)	50.0000	P_i^{out} (MW)	40.0000
	H_i^{in} (GJ/h)	0.0000	H_i^{out} (GJ/h)	50.0000
	G_i^{in} (km^3/h)	3.0382	G_i^{out} (km^3/h)	2.4306

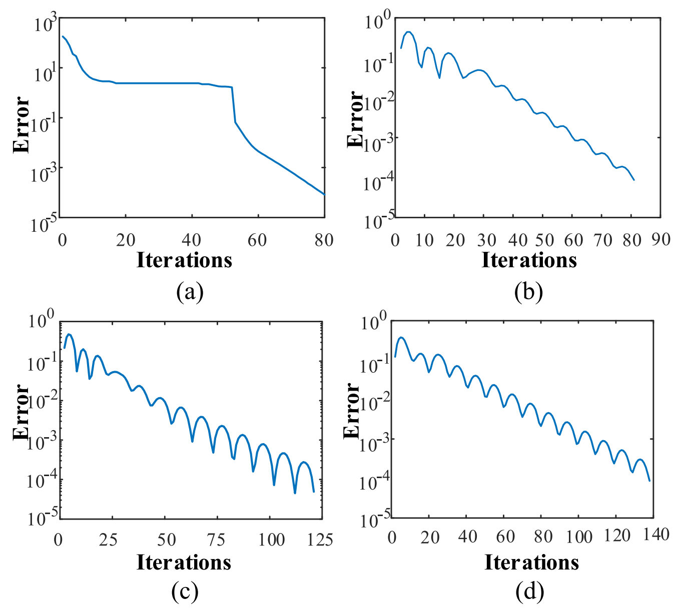

Fig. 3. Iteration process of the two algorithms. (a) ADMM algorithm. (b) DD algorithm by topology 1. (c) DD algorithm by topology 2. (d) DD algorithm by topology 3.

B. Solution Property

The results on the energy transformation by EHs are shown in Table III, where the input electricity and natural gas energy resources are complementarily transformed into electricity, natural gas, and heat energy resources. Take the EH 1 for illustration. Since the heat energy could only be transformed from other kinds of energy resources (i.e., electricity and natural gas), the optimal transformation is based on the cost functions of the energy resources. It can be found that a part of the input electricity (2.3189 MW) is used for direct electricity supply (1.8552 MW) and the rest is used to transform into heat energy. Similarly, a part of the input natural gas (1.6704 km^3/h) is used for direct gas supply (1.3363 km^3/h) and the rest is used to transform into heat energy. Hence, the heat energy of the EH 1 is transformed from 0.4637 MW electricity and 0.3341 km^3/h natural gas simultaneously.

C. Convergence Performance

For the two distributed algorithms, we will at first define the mismatch energy for different types of energy resources. The mismatched energy values $\Pi = \{P, H, G\}$ for ADMM and the proposed DD methods at the kth iteration are written as

$$e_{\text{ADMM}}^{\Pi,k} = \left|\Pi_L - \sum_{i=1}^{m} \Pi_i^{\text{out},k,ADMM}\right| \tag{80a}$$

$$e_{\text{DD}}^{\Pi,k} = \left|\Pi_L - \sum_{i=1}^{m} \Pi_i^{\text{out},k,DD}\right|. \tag{80b}$$

The convergence performance under the three topologies of the communication network is compared in Fig. 3, where the maximum mismatched value [$e_{\text{ADMM}}^{\Pi,k}$ in (80a)] is chosen as the error of ADMM while the relative deviation to the global optimal value is chosen as the error of DD method with a feasible initial solution because $e_{\text{DD}}^{\Pi,k}$should always be zero. It can be observed that topology 1 needs 81 iterations, topology 2 needs 121 iterations, and topology 3 needs 135 iterations. This suggests that less number of communication links will lead to more iterations for convergence. The reason is straightforward that more information can be exchanged at each iteration if there are more communication links and thus the convergence is performed better. Meanwhile,

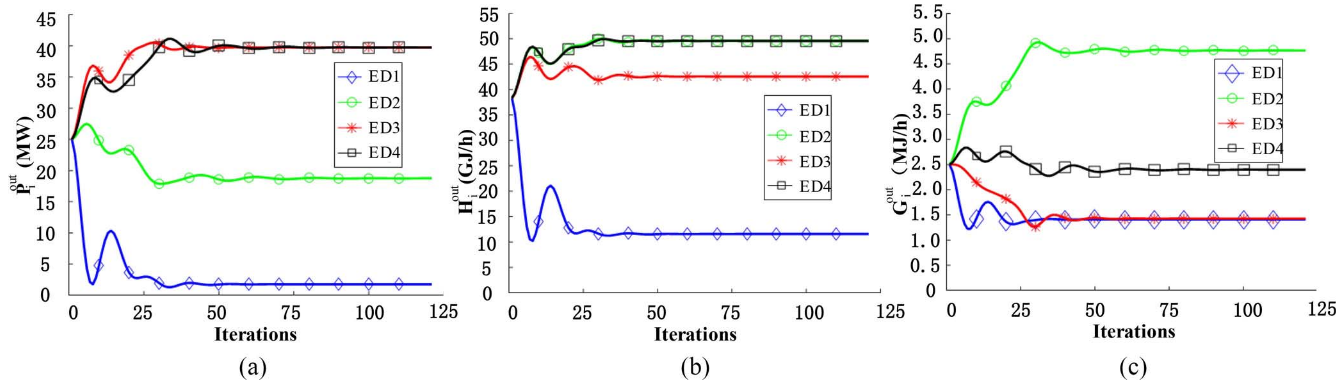

Fig. 4. Iteration process of the proposed DD method. (a) Electricity of EH outputs. (b) Heat of EH outputs. (c) Natural gas of EH outputs.

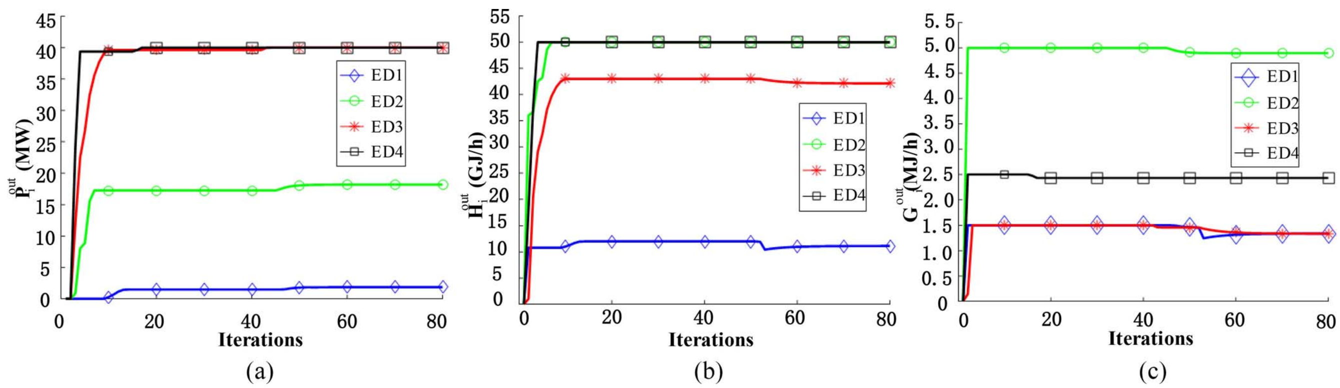

Fig. 5. Iteration process of the ADMM. (a) Electricity of EH outputs. (b) Heat of EH outputs. (c) Natural gas of EH outputs.

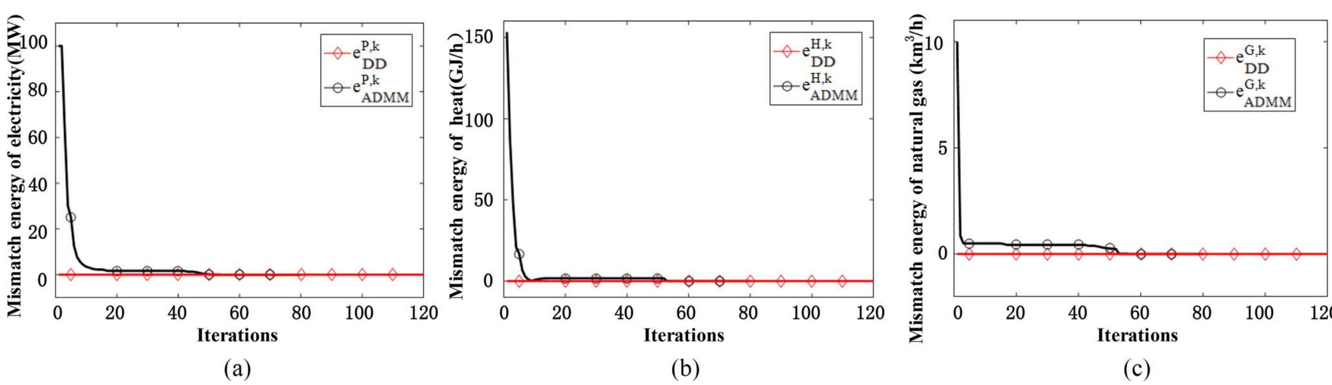

Fig. 6. Mismatch energy for different types of energy resource. Mismatch energy of (a) electricity, (b) heat, and (c) natural gas.

the ADMM algorithm needs 80 iterations, indicating that the proposed method needs more iterations for convergence than the ADMM algorithm. Note that, in the ADMM algorithm, any update of a variable requires the information of all other variables, so the topology of communication network must be the strongly connected graph (shaped like Topology 1).

Furthermore, the second communication topology is chosen to show the results of the proposed DD method and the ADMM, which are depicted in Figs. 4 and 5. It can be observed that the proposed method may have a larger oscillation during the iteration process than the ADMM algorithm. Again, from the comparison between Figs. 4 and 5, it observes that the proposed DD distributed algorithm actually needs more iterations than the traditional ADMM algorithm.

The formulation of the ADMM algorithm can be found in the Appendix. It generally cannot guarantee the feasibility at each iteration while the proposed DD method can strictly guarantee the feasibility during the iteration process. Fig. 6 depicts that before the convergence, the intermediate iteration of the ADMM is always infeasible. Accordingly, the algorithm converges once the feasibility is achieved. In contrast, the intermediate iteration of the proposed DD method is always feasible if and only if the initial solution is feasible. Moreover, the objective costs of the ADMM algorithm and the proposed DD method are 70890.61 ¥ and 70900.07 ¥, respectively. The optimal cost of the benchmark method (i.e., the centralized model) is 70893.76 ¥. Since the DD method is feasible at each step, it searches the optimal solution from the inner part of the feasible region (also known as, inner approximation), the final cost is slightly larger than that of the benchmark model. In contrast, the ADMM method is infeasible at each step, and it searches the optimal solution from the outer part of the feasible region (also known as, outer approximation), so the final cost is slightly smaller than that of the benchmark model. In general, the absolute errors of the two methods are both relatively small, i.e., smaller than 0.01%. It suggests that both the two methods can achieve the optimal value once the algorithms converge.

Finally, it was pointed out in [32] that the ADMM method cannot necessarily guarantee the convergence for the multi-block convex optimization. Fortunately, the proposed model in fact satisfies the sufficient condition in [32], so that the ADMM algorithm can converge. But there is still a question whether the ADMM algorithm can converge with additional local constraints while violating the sufficient condition in [32]. In contrast, the proposed DD is rigorously proven to be linearly convergent and strictly guarantee the feasibility at each step. This is the good convergence property of the proposed DD algorithm, but the oscillation is the price.

VI. Conclusion

This article proposed a DD-based distributed algorithm for the optimal control of m-IES. Some theorems and lemmas are given to prove that the proposed method can linearly converge to the optimal solution. The numerical results suggest that the proposed model can achieve the energy complementary by optimally dispatching multiple energy resources. For the proposed algorithm, less number of communication links will lead to more iterations for convergence. In addition, the comparison of the proposed method with the traditional ADMM, it shows that although the proposed method requires more iterations for convergence and has oscillation, it can strictly guarantee the feasibility at each iteration while the ADMM cannot guarantee the feasibility unless the optimal solution is achieved. Most importantly, there is still a question whether the ADMM algorithm can still converge with additional local constraints. In contrast, the proposed DD is rigorously proven to be linearly convergent for under mild conditions.

Appendix

The ADMM algorithm for the proposed optimization model (14), (15) can be formulated as

$$\begin{aligned}
L_{\rho_{\text{ADMM}}}(\mathbf{x}_1, \mathbf{x}_2, \ldots, \mathbf{x}_m, \mathbf{y}) &= \sum_{i=1}^{m} f_i^0(\mathbf{x}_i) + \mathbf{y}^T \mathbf{B}^T \mathbf{x} \\
&\quad + \frac{\rho_{\text{ADMM}}}{2} \left\| \mathbf{B}^T \mathbf{x} \right\|_2 \\
&= \sum_{i=1}^{m} f_i^0(\mathbf{x}_i) + \mathbf{y}^T \sum_{i=1}^{m} \mathbf{B}_i^T \mathbf{x}_i \\
&\quad + \frac{\rho_{\text{ADMM}}}{2} \left\| \sum_{i=1}^{m} \mathbf{B}_i^T \mathbf{x}_i \right\|_2 \\
\mathbf{x}_1^{k+1} &= \arg\min_{\mathbf{x}_1 \in \mathcal{H}_1} L_{\rho_{\text{ADMM}}} \\
&\quad \times \left(\mathbf{x}_1, \mathbf{x}_2, \ldots, \mathbf{x}_m^k, \mathbf{y}^k\right) \\
\mathbf{x}_2^{k+1} &= \arg\min_{\mathbf{x}_2 \in \mathcal{H}_1} L_{\rho_{\text{ADMM}}} \\
&\quad \times \left(\mathbf{x}_1^{k+1}, \mathbf{x}_2^k, \ldots, \mathbf{x}_m^k, \mathbf{y}^k\right) \\
&\vdots \\
\mathbf{x}_2^{k+1} &= \arg\min_{\mathbf{x}_m \in \mathcal{H}_m} L_{\rho_{\text{ADMM}}} \\
&\quad \times \left(\mathbf{x}_1^{k+1}, \mathbf{x}_2^{k+1}, \ldots, \mathbf{x}_m, \mathbf{y}^k\right) \\
\mathbf{y}^{k+1} &= \mathbf{y}^k + \rho_{\text{ADMM}} \sum_{i=1}^{m} \mathbf{B}_i^T \mathbf{x}_i^{k+1} \qquad (81)
\end{aligned}$$

where variables are updated to minimize the Lagrangian functions $L_{\rho_{\text{ADMM}}}(\mathbf{x}_1, \mathbf{x}_2, \ldots, \mathbf{x}_m, \mathbf{y})$ and the algorithm is stopped when the relaxed constraints $\mathbf{B}^T\mathbf{x} = 0$ are satisfied.

References

[1] K. Wang *et al.*, "A survey on energy Internet: Architecture, approach, and emerging technologies," *IEEE Syst. J.*, vol. 12, no. 3, pp. 2403–2416, Sep. 2018, doi: 10.1109/JSYST.2016.2639820.

[2] W. Wang, Y. Jiang, and W. Wu, "Multiagent-based resource allocation for energy minimization in cloud computing systems," *IEEE Trans. Syst., Man, Cybern., Syst.*, vol. 47, no. 2, pp. 205–220, Feb. 2017.

[3] G. Guandalini, S. Campanari, and M. C. Romano, "Power-to-gas plants and gas turbines for improved wind energy dispatchability: Energy and economic assessment," *Appl. Energy*, vol. 147, pp. 117–130, Jun. 2015.

[4] S. Clegg and P. Mancarella, "Integrated modeling and assessment of the operational impact of power-to-gas (P2G) on electrical and gas transmission networks," *IEEE Trans. Sustain. Energy*, vol. 6, no. 4, pp. 1234–1244, Oct. 2015.

[5] J. S. Kim and T. F. Edgar, "Optimal scheduling of combined heat and power plants using mixed-integer nonlinear programming," *Energy*, vol. 77, pp. 675–690, Dec. 2014.

[6] S. Murugan and B. Horák, "Tri and polygeneration systems—A review," *Renew. Sustain. Energy Rev.*, vol. 60, pp. 1032–1051, Jul. 2016.

[7] M. Mohammad, N. Younes, M. Behnam, and Y. Hossein, "Energy hub: From a model to a concept—A review," *Renew. Sustain. Energy Rev.*, vol. 80, pp. 1512–1527, Dec. 2017.

[8] S. Howell, H. Wicaksono, B. Yuce, K. McGlinn, and Y. Rezgui, "User centered neuro-fuzzy energy management through semantic-based optimization," *IEEE Trans. Cybern.*, vol. 49, no. 9, pp. 3278–3292, Sep. 2019.

[9] M. Brundage, Q. Chang, Y. Li, J. Arinez, and G. Xiao, "Implementing a real-time, energy-efficient control methodology to maximize manufacturing profits," *IEEE Trans. Syst., Man, Cybern., Syst.*, vol. 46, no. 6, pp. 855–866, Jun. 2016.

[10] C. Cheng, S. Tsao, and P. Lin, "SEEDS: A solar-based energy-efficient distributed server farm," *IEEE Trans. Syst. Man, Cybern., Syst.*, vol. 45, no. 1, pp. 143–156, Jan. 2015.

[11] A. Martinez-Mares and C. R. Fuerte-Esquivel, "A unified gas and power flow analysis in natural gas and electricity coupled networks," *IEEE Trans. Power Syst.*, vol. 27, no. 4, pp. 2156–2166, Nov. 2012.

[12] S. Chen, Z. Wei, G. Sun, K. W. Cheung, and Y. Sun, "Multi-linear probabilistic energy flow analysis of integrated electrical and natural-gas systems," *IEEE Trans. Power Syst.*, vol. 32, no. 3, pp. 1970–1979, May 2017.

[13] Y. Hu, H. Lian, Z. Bie, and B. Zhou, "Unified probabilistic gas and power flow," *J. Mod. Power Syst. Clean Energy*, vol. 5, no. 3, pp. 400–411, 2017.

[14] M. Aien, M. Rashidinejad, and M. Fotuhi-Firuzabad, "On possibilistic and probabilistic uncertainty assessment of power flow problem: A review and a new approach," *Renew. Sustain. Energy Rev.*, vol. 37, pp. 883–895, Sep. 2014.

[15] M. Andebili and H. Shen, "Price-controlled energy management of smart homes for maximizing profit of a GENCO," *IEEE Trans. Syst., Man, Cybern., Syst.*, vol. 49, no. 4, pp. 697–709, Apr. 2019.

[16] M. Faqiry and S. Das, "Double auction with hidden user information: Application to energy transaction in microgrid," *IEEE Trans. Syst., Man, Cybern., Syst.*, vol. 49, no. 11, pp. 2326–2339, Nov. 2019.

[17] Y. Jiang *et al.*, “Day-ahead stochastic economic dispatch of wind integrated power system considering demand response of residential hybrid energy system,” *Appl. Energy*, vol. 190, pp. 1126–1137, Mar. 2017.

[18] C. Liu, M. Shahidehpour, Y. Fu, and Z. Li, “Security-constrained unit commitment with natural gas transmission constraints,” *IEEE Trans. Power Syst.*, vol. 24, no. 3, pp. 1523–1536, Aug. 2009.

[19] C. Shao, X. Wang, M. Shahidehpour, X. Wang, and B. Wang, “An MILP-based optimal power flow in multicarrier energy systems,” *IEEE Trans. Sustain. Energy*, vol. 8, no. 1, pp. 239–248, Jan. 2017.

[20] A. Shabanpour-Haghighi and A. R. Seifi, “Simultaneous integrated optimal energy flow of electricity, gas, and heat,” *Energy Convers. Manag.*, vol. 105, pp. 579–591, Sep. 2015.

[21] J. Fang, Q. Zeng, X. Ai, Z. Chen, and J. Wen, “Dynamic optimal energy flow in the integrated natural gas and electrical power systems,” *IEEE Trans. Sustain. Energy*, vol. 9, no. 1, pp. 188–198, Jan. 2018.

[22] G. Sun, S. Chen, Z. Wei, and S. Chen, “Multi-period integrated natural gas and electric power system probabilistic optimal power flow incorporating power-to-gas units,” *J. Mod. Power Syst. Clean Energy*, vol. 5, pp. 415–423, Apr. 2017.

[23] Y. Li *et al.*, “Optimal stochastic operation of integrated low-carbon electric power, natural gas, and heat delivery system,” *IEEE Trans. Sustain. Energy*, vol. 9, no. 1, pp. 273–283, Jan. 2018.

[24] S. Wang, A. Taha, J. Wang, K. Kvaternik, and A. Hahn, “Energy crowdsourcing and peer-to-peer energy trading in blockchain-enabled smart grids,” *IEEE Trans. Syst., Man, Cybern., Syst.*, vol. 49, no. 8, pp. 1612–1623, Aug. 2019.

[25] H. Ahn, B. Kim, Y. Lim, B. Lee, and K. Oh, “Distributed coordination for optimal energy generation and distribution in cyber-physical energy networks,” *IEEE Trans. Cybern.*, vol. 48, no. 3, pp. 941–954, Mar. 2018.

[26] S. Boyd, N. Parikh, E. Chu, B. Peleato, and J. Eckstein, “Distributed optimization and statistical learning via the alternating direction method of multipliers,” *Found. Trends Mach. Learn.*, vol. 3, no. 1, pp. 1–122, 2010.

[27] T. Miyamoto, S. Kitamura, K. Mori, and Y. Izumi, “Distributed optimization using alternating direction method of multipliers,” *Appl. Energy Manag. Syst. Control Inf.*, vol. 60, no. 6, pp. 219–224, 2016.

[28] M. Ma, L. Fan, and Z. Miao, “Consensus ADMM and Proximal ADMM for economic dispatch and AC OPF with SOCP relaxation,” in *Proc. North Amer. Power Symp. (NAPS)*, Denver, CO, USA, 2016, pp. 1–6.

[29] T. Erseghe, “Distributed optimal power flow using ADMM,” *IEEE Trans. Power Syst.*, vol. 29, no. 5, pp. 2370–2380, Sep. 2014.

[30] J. Xu, H. Sun, and C. J. Dent, “ADMM-based distributed OPF problem meets stochastic communication delay,” *IEEE Trans. Smart Grid*, vol. 10, no. 5, pp. 5046–5056, Sep. 2019.

[31] S. Bolognani and S. Zampieri, “A distributed control strategy for reactive power compensation in smart microgrids,” *IEEE Trans. Autom. Control*, vol. 58, no. 11, pp. 2818–2833, Nov. 2013.

[32] C. Chen, B. He, Y. Ye, and X. Yuan, “The direct extension of ADMM for multi-block convex minimization problems is not necessarily convergent,” *Math. Program.*, vol. 155, pp. 57–79, Jan. 2016.

[33] T. T. Doan and A. Olshevsky, “On the geometric convergence rate of distributed economic dispatch/demand response in power networks,” 2016. [Online]. Available: arXiv:1609.06660.

[34] G. Qu and N. Li, “Harnessing smoothness to accelerate distributed optimization,” *IEEE Trans. Control Netw. Syst.*, vol. 5, no. 3, pp. 1245–1260, Sep. 2018, doi: 10.1109/TCNS.2017.2698261.

[35] J. Xu, S. Zhu, Y. C. Soh, and L. Xie, “Augmented distributed gradient methods for multi-agent optimization under uncoordinated constant stepsizes,” in *Proc. 54th IEEE Conf. Decis. Control*, Osaka, Japan, 2015, pp. 2055–2060.

[36] J. Xu, S. Zhu, Y. C. Soh, and L. Xie, “A Bregman splitting scheme for distributed optimization over networks,” *IEEE Trans. Autom. Control*, vol. 63, no. 11, pp. 3809–3824, Nov. 2018.

[37] N. Ul Hassan, C. Yuen, and D. Niyato, “Blockchain technologies for smart energy systems: Fundamentals, challenges, and solutions,” *IEEE Ind. Electron. Mag.*, vol. 13, no. 4, pp. 106–118, Dec. 2019.

[38] M. F. Zia, M. Benbouzid, E. Elbouchikhi, S. M. Muyeen, K. Techato, and J. M. Guerrero, “Microgrid transactive energy: Review, architectures, distributed ledger technologies, and market analysis,” *IEEE Access*, vol. 8, pp. 19410–19432, 2020.

[39] J. Xu, S. Zhu, Y. C. Soh, and L. Xie, “A dual splitting approach for distributed resource allocation with regularization,” *IEEE Trans. Control Netw. Syst.*, vol. 6, no. 1, pp. 403–414, Mar. 2019.

[40] S. Boyd and L. Vandenberghe, *Convex Optimization*, 1st ed. Cambridge, U.K.: Cambridge Univ. Press, 2004, ch. 3, sec. 1, p. 71.

[41] A. Sheikhi, A. Ranjbar, and H. Oraee, “Financial analysis and optimal size and operation for a multicarrier energy system,” *Energy Build*, vol. 48, pp. 71–78, May 2012.

[42] A. Maroufmashat *et al.*, “Modeling and optimization of a network of energy hubs to improve economic and emission considerations,” *Energy*, vol. 93, pp. 2546–2558, Dec. 2015.

Ming Qu (Student Member, IEEE) received the B.S. degree in electrical engineering from the School of Electrical Engineering, Shandong University, Jinan, China, in 2017. He is currently pursuing the Ph.D. degree with Xi’an Jiaotong University, Xi’an, China.

His major research interests include power system optimization and renewable energy integration.

Tao Ding (Senior Member, IEEE) received the B.S.E.E. and M.S.E.E. degrees in electrical engineering from Southeast University, Nanjing, China, in 2009 and 2012, respectively, and the Ph.D. degree in electrical engineering from Tsinghua University, Beijing, China, in 2015.

In 2013 and 2014, he was a Visiting Scholar with the Department of Electrical Engineering and Computer Science, University of Tennessee, Knoxville, TN, USA. He is currently an Associate Professor with the State Key Laboratory of Electrical Insulation and Power Equipment, School of Electrical Engineering, Xi’an Jiaotong University, Xi’an, China. His current research interests include electricity markets, power system economics and optimization methods, and power system planning and reliability evaluation.

Dr. Ding received the Excellent Master and Doctoral Dissertation from Southeast University and Tsinghua University, respectively, and the Outstanding Graduate Award of Beijing City. He has published more than 60 technical papers and authored by “Springer Theses” recognizing outstanding Ph.D. research around the world and across the physical sciences—*Power System Operation With Large Scale Stochastic Wind Power Integration*. He is an Editor of the IEEE TRANSACTIONS ON POWER SYSTEMS, *IET Generation, Transmission & Distribution*, and *CSEE Journal of Power and Energy Systems*.

Wenhao Jia (Student Member, IEEE) received the B.S. degree in electrical engineering from the School of Electrical Engineering, Xi’an Jiaotong University, Xi’an, China, in 2020, where he is currently pursuing the M.S. degree.

His major research interests include power system optimization and renewable energy integration.

Shanying Zhu (Member, IEEE) received the B.S. degree in information and computing science from the North China University of Water Resources and Electric Power, Zhengzhou, China, in 2006, the M.S. degree in applied mathematics from the Huazhong University of Science and Technology, Wuhan, China, in 2008, and the Ph.D. degree in control theory and control engineering from Shanghai Jiao Tong University, Shanghai, China, in 2013.

From 2013 to 2015, he was a Research Fellow with the School of Electrical and Electronic Engineering, Nanyang Technological University, Singapore, and also with the Berkeley Education Alliance for Research in Singapore, Singapore. In 2015, he joined Shanghai Jiao Tong University, where he is currently an Associate Professor with the Department of Automation. His research interests include multiagent systems and wireless sensor networks, particularly in coordination control of mobile robots and distributed detection and estimation in sensor networks and their applications in industrial networks.

Yongheng Yang (Senior Member, IEEE) received the B.Eng. degree in electrical engineering and automation from Northwestern Polytechnical University, Shaanxi, China, in 2009, and the Ph.D. degree in electrical engineering from Aalborg University, Aalborg, Denmark, in 2014.

He was a postgraduate student with Southeast University, Nanjing, China, from 2009 to 2011. In 2013, he spent three months as a Visiting Scholar with Texas A&M University, College Station, TX, USA. He is currently an Associate Professor with the Department of Energy Technology, Aalborg University, where he also serves as the Vice Program Leader for the research program on photovoltaic systems. His current research is on the integration of grid-friendly photovoltaic systems with an emphasis on the power electronics converter design, control, and reliability.

Dr. Yang was a recipient of the 2018 *IET Renewable Power Generation* Premium Award and was an Outstanding Reviewer for the IEEE TRANSACTIONS ON POWER ELECTRONICS in 2018. He is the Chair of the IEEE Denmark Section. He serves as an Associate Editor for several prestigious journals, including the IEEE TRANSACTIONS ON INDUSTRIAL ELECTRONICS, IEEE TRANSACTIONS ON POW ER ELECTRONICS, and the IEEE Industry Applications Society (IAS) Publications. He is a Subject Editor of *IET Renewable Power Generation* for Solar Photovoltaic Systems, including the Maximum Power Point Tracking.

Frede Blaabjerg (Fellow, IEEE) received the Ph.D. degree in electrical engineering from Aalborg University, Aalborg, Denmark, in 1995. He is currently pursuing the *honoris causa* degree with University Politehnica Timisoara, Timişoara, Romania, and Tallinn Technical University, Tallinn, Estonia.

He was with ABB-Scandia, Randers, Denmark, from 1987 to 1988. From 1988 to 1992, he became an Assistant Professor in 1992, an Associate Professor in 1996, and a Full Professor of power electronics and drives in 1998. In 2017, he became a Villum Investigator. He has published more than 600 journal papers in the fields of power electronics and its applications. He is the co-author of four monographs and editor of ten books in power electronics and its applications. His current research interests include power electronics and its applications, such as in wind turbines, PV systems, reliability, harmonics, and adjustable speed drives.